QUANTIFYING GLOBAL PLASMASPHERIC IMAGES WITH *IN SITU* OBSERVATIONS

M. B. MOLDWIN
Institute of Geophysics and Planetary Physics and Department of Earth and Space Sciences, UCLA, Los Angeles CA 90095-1567 USA

B. R. SANDEL
Lunar and Planetary Laboratory, University of Arizona, Tucson AZ

M. F. THOMSEN and R. C. ELPHIC
Los Alamos National Laboratory, Los Alamos, NM

Abstract. Simultaneous IMAGE EUV plasmaspheric images and Magnetospheric Plasma Analyzer (MPA) data from the Los Alamos National Laboratory's geosynchronous satellites are combined to understand plasmaspheric behavior and to quantify the global images. A brief review of the understanding of the plasmasphere as learned from in situ observations prior to the launch of IMAGE is given to place the results presented here into context.

Keywords: plasmasphere, plasmapause, EUV

1. Introduction: Understanding of Plasmasphere Prior to IMAGE

The plasmasphere and the plasmapause have been studied using spacecraft in many different orbits (polar, geosynchronous and near-equatorial elliptical) and with a variety of instruments (plasma wave instruments, plasma analyzers, and spacecraft potential probes) (e.g., Gringauz, 1963; Chappell et al., 1970; Decreau et al., 1982; Horwitz et al., 1986; Carpenter and Anderson, 1992; Moldwin et al., 1994; Sheeley et al., 2001). The picture developed from these diverse observations showed a plasmasphere that decreased in size with increasing geomagnetic activity and often showed a dusk side bulge region. This bulge region was found to shift towards noon with increasing geomagnetic activity and shift past dusk with low levels of steady geomagnetic activity (e.g., Higel and Wu, 1984, Moldwin et al., 1994). Essentially all of these studies defined the plasmapause as the region of sharp density gradient. This gradient was often a factor of five to 10 in under 0.5 L. A theoretical understanding of this behavior was developed soon after the discovery of the plasmapause by Carpenter, (1963) and Gringauz, (1963). The model describes the plasmapause as the last closed equipotential of the combination of the convection and corotation electric fields (Nishida, 1966; Brice, 1967; Dungey, 1967). Figure 1, (from Brice, 1967), shows the potential lines in the equatorial plane.

The plasmapause in this model is the last equipotential line that completely closes around the Earth. Plasma on flux tubes earthward of this line corotates with

Space Science Reviews **109:** 47–61, 2003.

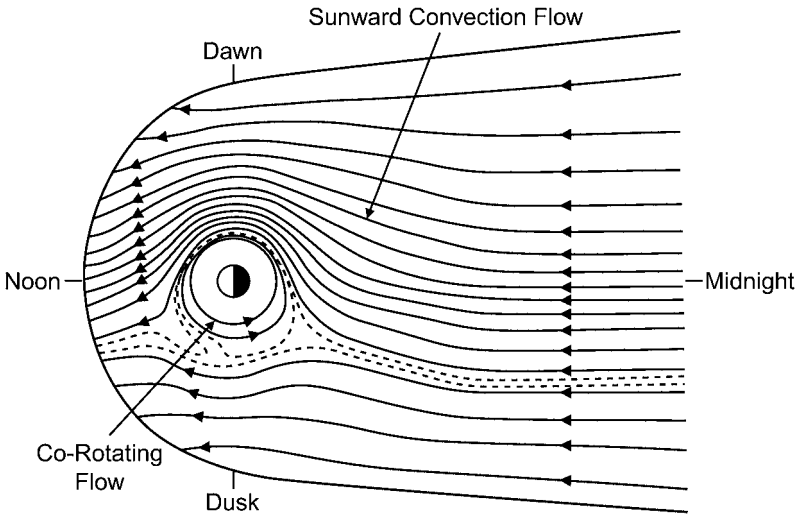

Figure 1. The equatorial convection flow stream-lines for low energy plasma showing the interaction of the sunward convection and corotation. The dashed lines show the boundary between open and closed drift trajectories. [Figure adapted from (Brice, 1967)].

the Earth allowing upflowing ionospheric plasma to accumulate. On flux tubes on the other side of this last closed equipotential line, the drift trajectories move sunward and are eventually lost to the magnetopause and boundary layer. These flux tubes therefore do not have time to accumulate significant plasma and are hence lower density than the flux tubes that can corotate many days. The size and shape of the plasmapause predicted with this model fits observations to zeroth order. However, observations continually have shown that this simple model is only correct on the average. Significant plasmaspheric structure and deviations from this model are routine. This is due to a number of reasons. One possible reason is that a steep density gradient formed earlier due to enhanced convection can have a lifetime comparable to the refilling rate. Therefore during the recovery period following an interval of enhanced convection, the last closed equipotential will be farther from the Earth than the plasmapause as defined by the inner most steep gradient (Moldwin et al., 2002). Another complication is the formation of plasma tails or drainage plumes that often form in the dusk sector and can either remain fairly stationary in local time or "wrap" around the plasmasphere as it corotates toward midnight (e.g., Chen et al., 1976). Finally, there can be significant density structure at the plasmapause due to local instabilities, ULF waves, and locally confined regions of intense electric fields (e.g., Carpenter et al., 1993, 2000). These time variable phenomena all contribute to developing a complex and dynamic plasmapause.

It should be noted that the term "plasmapause"can have different meanings depending on the context. The plasmapause has been defined as the steep density gradient (e.g., Carpenter, 1963); transition from cold and isotropic to warm and

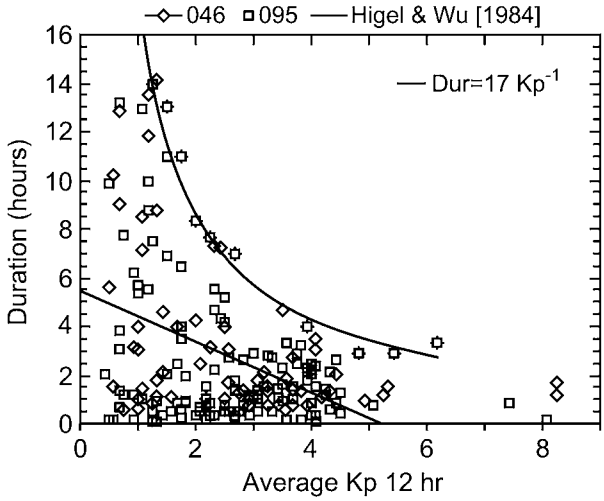

Figure 2. The duration of plasmaspheric intervals as observed by two LANL geosynchronous spacecraft (1989-046 and 1990-095) as a function of average *Kp* over the 12 hours prior to observations [From Moldwin et al., (1994)].The straight line is the best fit line found by Higel and Wu (1984) for this same relationship. The curved line shows that the maximum duration of plasmaspheric-like plasma follows a Kp^{-1} relationship.

field-aligned distributions (e.g., Horwitz et al., 1986; Moldwin et al., 1995); or the theoretical last closed equipotential boundary (e.g., Nishida, 1966).

1.1. GEOSYNCHRONOUS PICTURE

The plasmaspheric bulge region has been studied using the GEOS 2 and Los Alamos National Laboratory geosynchronous satellites among others. Observations of the cold plasma density at synchronous orbit shows that plasmaspheric-like plasma is observed essentially everyday but with highly variable durations and local time extents. However, most often the plasmaspheric-like plasma is observed in the dusk sector for duration of two hours or less. Higel and Wu (1984) and Moldwin et al. (1994) examined the structure of the plasmaspheric-like plasma and found systematic behavior in the duration and local time of occurrence. In these studies, plasmaspheric-like intervals were defined when the density exceeded 10 cm^{-3}. Figure 2, from Moldwin et al. (1994), shows the observed duration of plasmaspheric plasma (in hours) observed from two LANL geosynchronous satellites as a function of *Kp* averaged over the previous 12 hours. Note that the duration of the plasmaspheric-like plasma at geosynchronous orbit decreases with increasing geomagnetic activity as represented by *Kp*. However, for $Kp \leq 2$ the duration can essentially have any length, though intervals of continuously observed plasmaspheric-like plasma greatly increases.

Figure 3 shows the LT mid-point of the plasmaspheric-like plasma as a function of *Kp*. Note that the plasmaspheric-like plasma at synchronous orbit is most

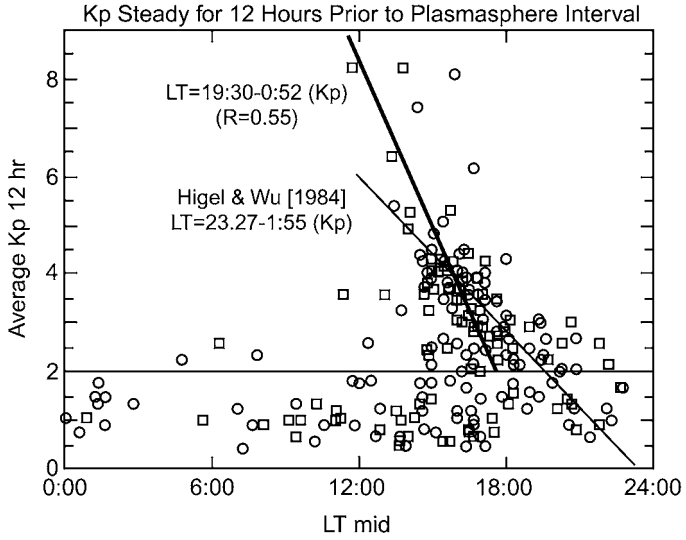

Figure 3. The mid-point in local time of the plasmaspheric observations from two LANL geosynchronous spacecraft as a function of average *Kp* over the 12 hours prior to observation [From Moldwin et al. (1994)]. The thin straight line is the best fit line found by Higel and Wu (1984), whereas the thick line is the best fit for these data points for $Kp \geq 2$.

often observed at dusk but the mid-point moves towards noon with increasing geomagnetic activity. This behavior was shown to be the typical response of the duskside plasmasphere following geomagnetic storms. Elphic et al. (1996) performed a superposed epoch analysis of the plasmaspheric plasma observations at geosynchronous orbit using the time of sudden storm commencent (SSC) as the t $= 0$ fiducial.

Figure 4 shows a schematic derived from their results. Note that the plasmaspheric plasma systematically shifts towards noon in direct response to the storm-time electric fields.

One of the puzzles that evolved from observations of plasmaspheric-like plasma observed at geosynchronous orbit using multiple geosynchronous satellites was that often spacecraft would observe the plasmaspheric-like plasma at different locations and for different durations even when the spacecraft were separated by only a few hours in local time. It was suggested that either there were dynamics at length-scales of a few hours even during steady geomagnetic conditions, that there was structure as a function of latitude (since the magnetic inclination of the geographically equatorial spacecraft could range from about ± 11 degrees depending on the longitude of the spacecraft), or that some small scale features corotate with the spacecraft while others do not.

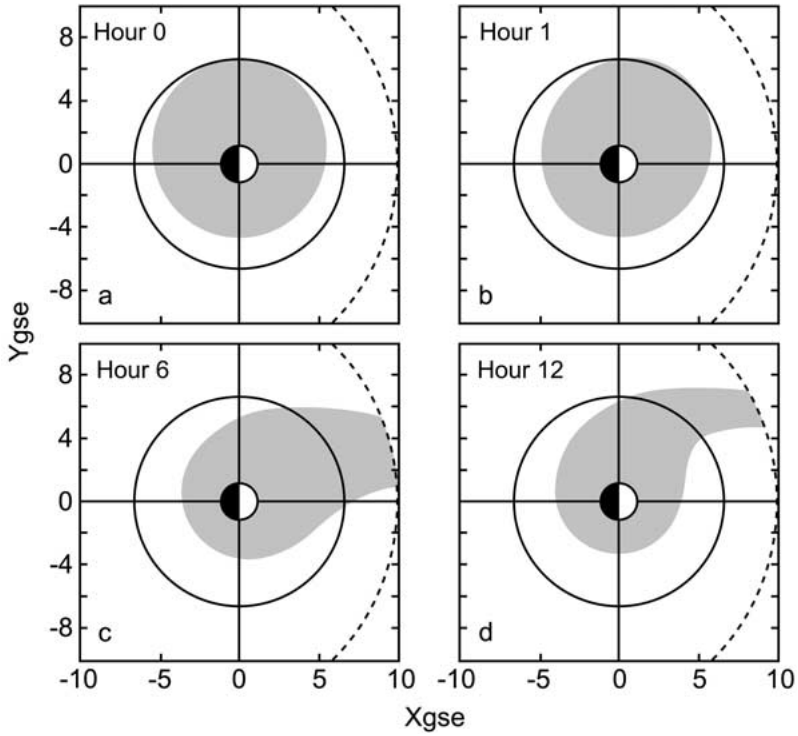

Figure 4. A schematic showing the inferred behavior of the outer plasmasphere following a geomagnetic storm [From Elphic et al. (1996)]. Note that the plasmaspheric-plasma that crosses geosynchronous orbit shifts towards noon and has shorter duration immediately following the SSC.

1.2. EQUATORIAL PICTURE

Satellites with elliptical orbits with a wide range of apogees and inclinations have observed the sharp density gradient of the plasmasphere and have been used to develop statistical pictures and models of the shape and dynamics of the plasmapause. This brief review will summarize only two of these studies: the ISEE 1/2 study of Carpenter and Anderson, (1992) and the more recent Moldwin et al., (2002) study that used CRRES observations. Both studies defined the plasmapause as the inner most sharp density gradient where the density must have changed by a factor of 5 within 0.5 L. The ISEE dataset consisted of a little over 200 plasmapause observations whereas the CRRES dataset contained nearly 1000 plasmapause crossings. Both sets had their observations distributed in local time and extended out to around an *L shell* of 7. These studies binned their observations as a function of geomagnetic activity history, with Carpenter and Anderson (1992) using the maximum *Kp* value that appeared in the previous 24 hours with some delay imposed for dayside observations. Moldwin et al. (2002) used the maximum *Kp* that occurred in the previous 12 hours with no delay imposed for dayside observations. Both studies found that the plasmasphere was essentially circular on average and had its radial

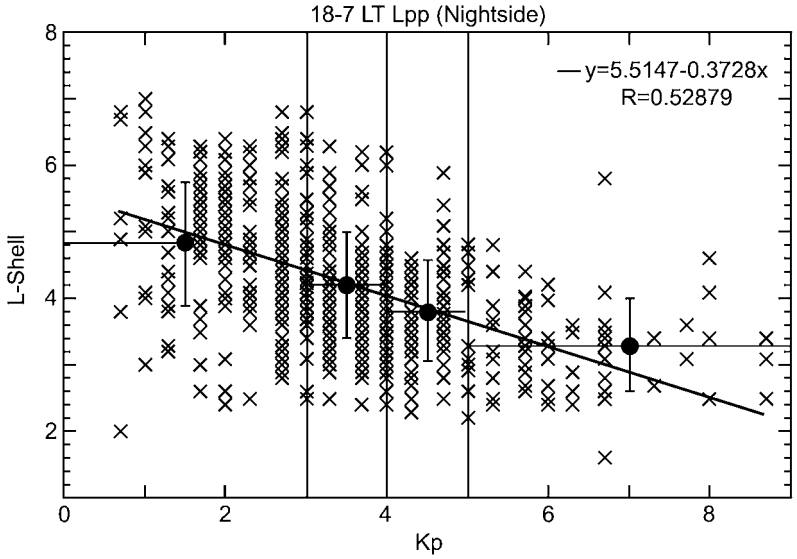

Figure 5. The location of the plasmapause as observed by CRRES on the nightside of the Earth. The large points with error bars are the mean position as a function of 4 broad *Kp* bins. The error bars show the width of the *Kp* bin and the standard deviation of the plasmapause locations in that bin. The best-fit line through the data points is given [From (Moldwin et al., 2002)].

distance vary linearly with *Kp*. The Moldwin et al. study explicitly calculated the variability of the best-fit lines and found that the plasmapause position typically varies up to an *L Shell* even during steady geomagnetic conditions. The Carpenter and Anderson model, though not continuous in local time, is probably the most widely used plasmapause location model (e.g., see Gallagher et al., 1998). Unfortunately, the linear fit model is often taken as "gospel" despite the warnings given by the authors. One such warning given by Carpenter (1969) reads:

> The results presented above may be deceptive in their simplicity. Data not presented here indicate that the plasmapause is extremely complex, with regions or irregular behavior, periods of rapid expansion or compression, and variations in details of the plasma profile at the boundary.

Despite these warnings, the plasmapause is often represented as a smooth boundary that changes its size linearly with changing geomagnetic activity. As Figure 5 shows, the plasmapause position has a wide variability as a function of geomagnetic activity. For low geomagnetic activity levels ($Kp \leq 2$), and in the dusk sector, the plasmapause can essentially be located at a wide range of radial distances.

1.3. Variability in Density and Structure is the Rule

Several studies on the variability of plasmaspheric density structure were done with both geosynchronous and elliptical orbiting spacecraft. LeDocq et al. (1994) used

CRRES plasma wave data and Moldwin et al. (1995) using the LANL geosynchronous MPA data showed that there was often density structure observed at the smallest observable length scales and that the plasmaspheric-like plasma was often a combination of cold isotropic plasma and warmer field-aligned plasma. Saturated flux tubes often only contained the cold isotropic population, whereas the trough or refilling plasmaspheric flux tubes often contained a combination of isotropic and warmer field-aligned populations. The study of Moldwin et al. (2002) demonstrated that the plasmapause profile often is very complex and that the "classic" clean plasmaspheric density profile is actually fairly rare, being observed on only 13% of the CRRES plasmapause examples. Figure 6 shows two examples of more typical plasmaspheric profiles observed by CRRES.

1.4. Simple and Incorrect Picture

These earlier in situ studies showed that the simple teardrop convection model of the plasmasphere was highly simplified and did not represent the true location or structure of the plasmapause. We now know that the plasmasphere and plasmapause location generally follow trends in geomagnetic activity but that the history of that activity, the occurrence of both substorms and storms, and the interaction with waves and ring current particles can have a significant impact on the fine and meso-scale structure of the plasmapause. From these studies a number of open questions remained with regards to the structure and dynamics of the plasmasphere. These include:

- What features corotate? Under what conditions? Which features are relatively stable in local time?
- What is the relationship between the geosynchronous observations and the plasmapause as measured with elliptical spacecraft?

With the launch of IMAGE, these questions can be addressed and preliminary answers to these questions are given below.

2. Methodology

This study combines observations from the IMAGE EUV imager with *in situ* cold ion observation from the Magnetospheric Plasma Analyzer onboard several LANL geosynchronous satellites. The IMAGE EUV instrument provides the first global images of the plasmasphere and can be used to follow the dynamics of the plasmapause (Sandel et al., 2001). The multiple geosynchronous satellites that carry the MPA instruments (McComas et al., 1993) can provide the plasma density at several places in the inner magnetosphere simultaneously to the IMAGE EUV picture. We can quantify the IMAGE EUV picture by determining the location of the plasmapause and the intensity of the emission as a function of local time and radial distance. This can then be compared to the measured *in situ* number density.

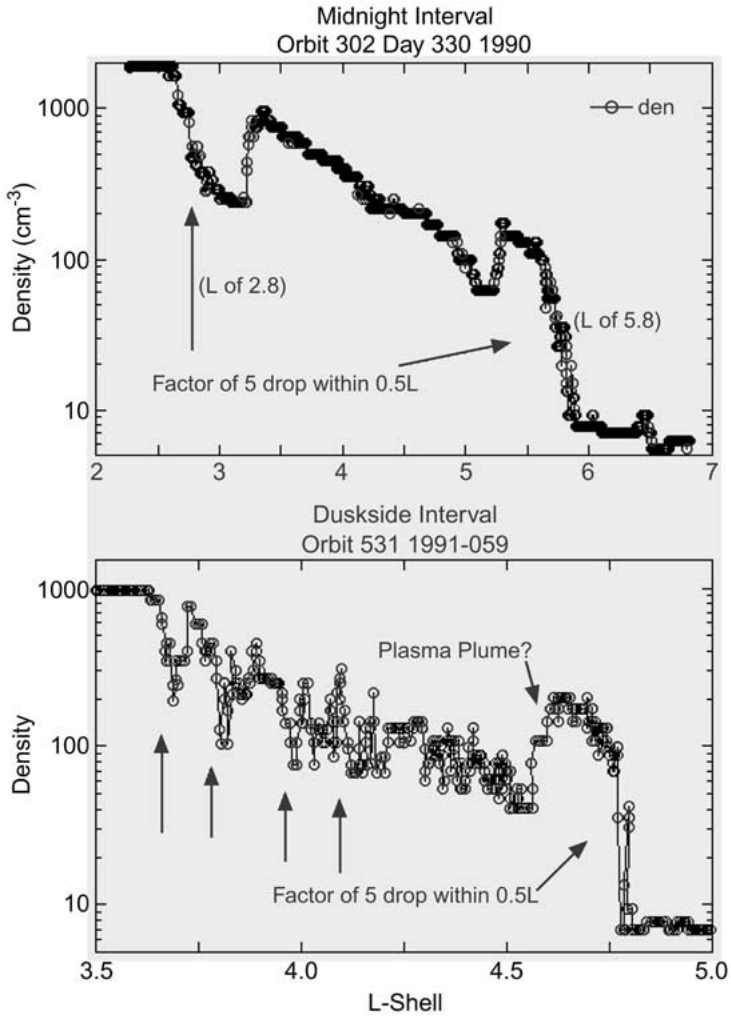

Figure 6. Two examples of "typical" plasmapause crossings as seen by CRRES. A majority of plasmapause observations showed structure at or beyond the inner most steep density gradient [From Moldwin et al., 2002]. The figures show the density as a function of *L shell* on a semi-log plot.

3. Observations

This study examines two intervals in detail. The first interval is from the May 24, 2000 storm. During this time, three LANL satellites observed plasmaspheric plasma in the noon-dusk quadrant while the IMAGE EUV pictures indicated the presence of a plasmaspheric plume in the same sector. Figure 7 is the 1994-084 time-energy spectrogram for this interval with the different magnetospheric regions labeled. The figure shows the ion flux (top panel) and electron flux (bottom panel) as a function of energy. The vertical axis is a log scale of energy from 1 eV to

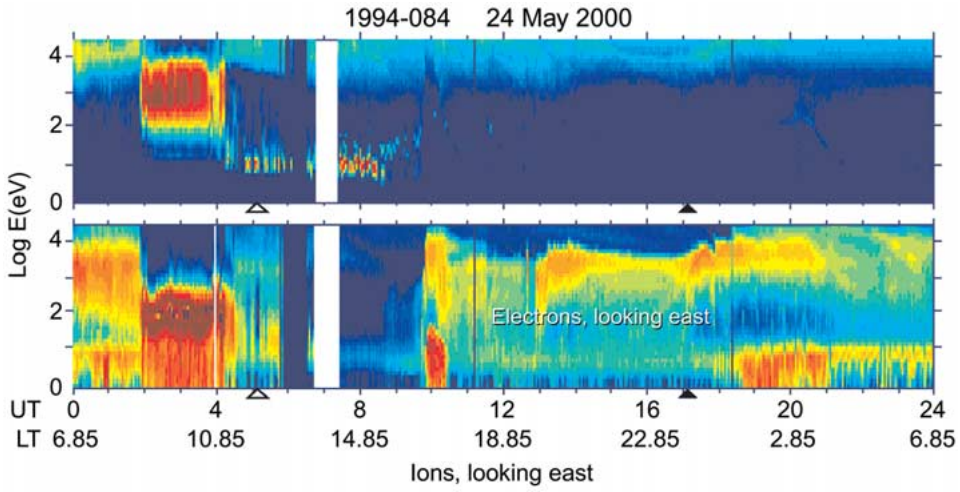

Figure 7. A time-energy spectrogram of 1994-084 MPA ion and electron data for May 24, 2000. The different plasma regions are labeled.

40 keV. The figure shows one day of data with the horizontal axis showing the UT (with LT in parenthesis). The open triangle shows local noon, while the filled in triangles show local midnight. The color scale indicates flux level with high fluxes represented by red. Note the presence of plasmaspheric plasma extending from just prior to noon to late afternoon as indicated by the intense fluxes of low energy ions. The magnetosheath (as indicated by the presence keV ions and 100s of eV electrons) was observed prior to the plasmaspheric interval indicating that the solar wind dynamic pressure had moved the magnetopause inside synchronous orbit. The plasmaspheric plasma that was observed on May 25 (not shown) has moved to later local times indicative of the recovery of the plasmasphere (see Figure 4 above) and had a shorter local time extent.

IMAGE EUV observed a plasmaspheric plume that appeared to extend to near synchronous on both of these days as well. Figure 8 shows the IMAGE pictures from May 24 and 25 side-by-side from similar perspectives. IMAGE EUV observes resonantly scattered sunlight at 30.4 nm. The sharp edge to the bright emissions is identified as the plasmapause. This sharp edge in the EUV emission is mapped to the equatorial plane in the panels below the images. The plume is more extensive on May 24 compared to the 25th and the plume has rotated away from noon towards dusk. These observations are consistent with the geosynchronous in situ data and demonstrate that the synchronous orbit "bulge" is a plasma plume or tail as predicted by Grebowsky (1970).

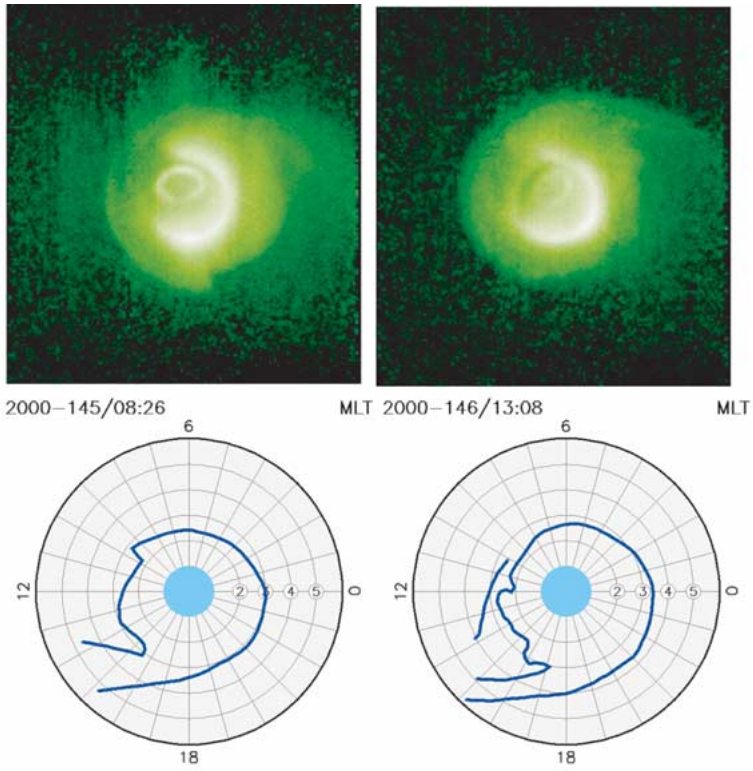

Figure 8. The IMAGE EUV observations of the plasmasphere and its duskside plume on May 24 and 25, 2000. The Earth is at the center of both images (the auroral oval can also be seen). Local midnight is to the left along the "Earth's shadow". In the bottom two panels the edge of the bright EUV emmission is mapped to the equatorial plane, now with midnight to the right. This mapping shows that the plume became narrower and shifted in local time towards dusk over this interval.

4. Quiet Times

A second interval was selected to study times when geosynchronous orbit spacecraft observe plasmaspheric plasma for extended ($\geq$18 hours) periods. In particular, we are interested in understanding if these plasmaspheric intervals are due to a global expansion of the plasmasphere beyond synchronous orbit or whether they are due to meso-scale bulges co-rotating giving the appearance that the plasmasphere extends beyond synchronous. On May 2, 2001 geomagnetic activity was steady and low (*Kp* for May 1 and 2 ranged from 0+ to 2). The LANL satellites observed plasmaspheric-like plasma for extended periods and the IMAGE EUV observed an expanded plasmasphere as well. Figure 9 shows a radial cut across an EUV image similar to the ones in Figure 8 for this interval. The intensity is mapped assuming a dipole field model. This method is done at several local time sectors in order to map out the plasmapause location as a function of local time.

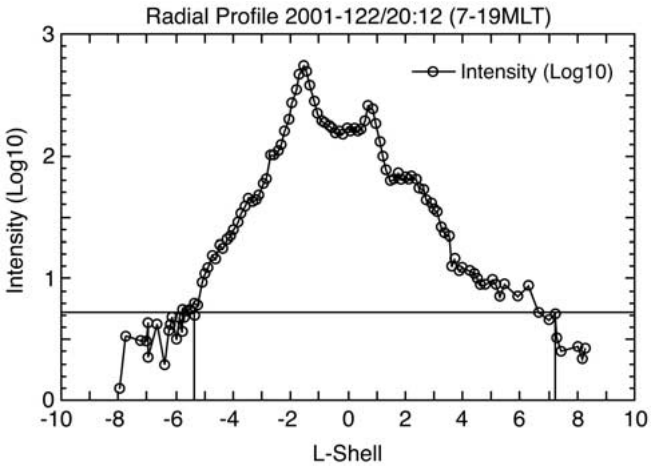

Figure 9. A radial cut in *L Shell* from 7 to19 MLT of the intensity of the IMAGE EUV counts for the May 2, 2001 20:12UT image. The vertical lines mark the estimated plasmaspause location using the background count rate as the threshold.

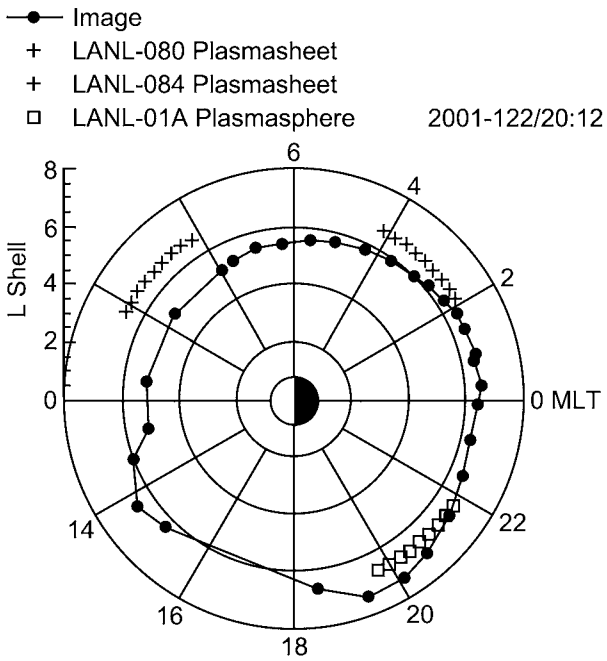

Figure 10. The inferred location of the IMAGE EUV plasmapause overlayed with the plasma regime simultaneously observed by the three LANL MPA spacecraft. Note that the IMAGE EUV data implies a duskside bulge extending beyond synchronous orbit which agrees with the in situ observations.

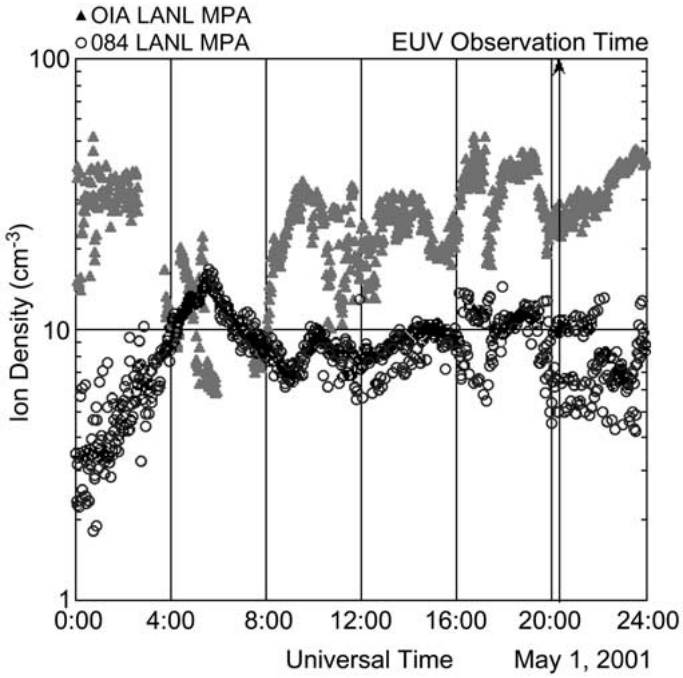

Figure 11. The observed *in situ* density of the three LANL MPA spacecraft at the time of IMAGE EUV observation showing that the threshold for IMAGE intensity is about 40 ions cm^{-3}.

Figure 10 shows the results of this mapping. The IMAGE picture shows that there is a slight duskside bulge that extends beyond synchronous orbit. Superimposed on this map are the observations from three LANL spacecraft ± 1 hr about the time of the IMAGE EUV observation. The two spacecraft located on the dawnside observe refilling trough densities whereas the LANL spacecraft at dusk observes plasmaspheric plasma. These observations agree with the plasmapause location estimates from IMAGE.

Figure 11 shows the measured *in situ* densities for the three LANL spacecraft on this day. The lowest EUV intensities detected within the plasmasphere correspond to densities of about 30 to 40 ions cm^{-3}. Of course, since the IMAGE EUV observations are a line-of-sight measurement, the minimum intensity is also a function of the path length through the plasmasphere. However, this volume density gives a rough estimate of the *in situ* densities needed at the edge of the plasmasphere. This threshold ion density is the same as inferred by Goldstein et al., (2002), who compared EUV images with electron density measurements made by the IMAGE Radio Plasma Imager. It is also consistent with the same authors' estimate of the threshold based on the observed noise background and the EUV sensitivity.

5. Conclusions

The global images from IMAGE EUV allows for the first time the direct comparison of the time-evolving global structure of the plasmasphere with multiple *in situ* plasma observations. Both sets of observations show that there can be significant (± 1 L Shell) variability in the radial location of the plasmapause as a function of local time for a given level of geomagnetic activity. There seems to be good correspondence between the EUV images inferred plasmasphere and *in situ* observations. Finally, the EUV images have shown that there are radial structures that corotate and those (most notably duskside plume features) that can be rather stagnant. Therefore the frequently-observed lack of correspondence between two closely spaced LANL geosynchronous satellites appears to be due to one satellite following a corotating density feature.

Acknowledgements

The authors thank both referees for their kind comments and constructive criticism. M.B.M. thanks J. Burch for the invitation to present this paper at the 2002 Yosemite Conference.

References

Anderson, R.R., Gurnett, D.A., and Odem, D.L.: 1992, 'CRRES plasma wave experiment', *J. Spacecraft and Rockets* **29**, 570.

Borovsky J.E., Thomsen, M.F., and McComas, D.J.: 1997, 'The superdense plasma sheet: Plasmaspheric origin, solar wind origin, or ionospheric origin?', *J. Geophys. Res.* **102**, 22089.

Brice, N.M.: 1967, 'Bulk motion of the magnetosphere', *J. Geophys. Res.* **7**, 5193.

Carpenter, D.L.: 1963, 'Whistler evidence of a "knee" in the magnetospheric ionization density profile', *J. Geophys. Res.* **68**, 1675.

Carpenter, D.L., Park, C.G., Taylor, H.A. and Brinton, H.C.: 1969, 'Multi-experiment detection of the plasmapause from EOGO satellites and Antarctic ground stations', *J. Geophys. Res.* **74**, 1837.

Carpenter, D.L., and Anderson, R.R., 'An ISEE/Whistler model of equatorial electron density in the magnetosphere', *J. Geophys. Res.* **97**, 1097.

Carpenter, D.L., Giles, B.L., Chappell, C.R., Decrau, P.M.R, Anderson, R.R., Persoon, A.M., Smith, A.J., Corcuff, Y., and Canu, P.: 1993, 'Plasmasphere dynamics in the duskside bulge: A new look at an old topic', *J. Geophys. Res.* **98**, 19243.

Carpenter, D.L., Anderson, R.R., Calvert, W., and Moldwin, M.B.: 2000, 'CRRES observations of density cavities inside the plasmasphere', *J. Geophys. Res.* **105**, 23323.

Chappell, C.R.: 1974, 'Detached plasma regions in the magnetosphere', *J. Geophys. Res.* **79**, 1861.

Chappell, C.R., Harris, K.K., and Sharp, G.W.: 1970, 'The morphology of the bulge region of the plasmasphere', *J. Geophys. Res.* **75**, 3848.

Chappell, C.R.: 1971, 'The dayside of the plasmasphere', *J. Geophys. Res.* **76**, 7632.

Chen, A.J., Grebowsky, J.M., and Marubashi, K.: 1976, 'Diurnal variation of thermal plasma in the plasmasphere', *Planet. Space Sci.* **24**, 765.

Decreau, P.M.E., Beghin, C., and Parrot, M.: 1982, 'Global characteristics of the cold plasma in the equatorial plasmapause region as deduced from the GEOS 1 mutual impedance probe', *J. Geophys. Res.* **87**, 695.

Doe, R.A., Moldwin, M.B., and Mendillo, M.: 1992, 'Plasmapause morphology determined from an empirical ionospheric convection model', *J. Geophys. Res.* **97**, 1151.

Dungey, J.W.: 1967, 'The theory of the quiet magnetosphere', in *Proceedings of the 1966 Symposium on Solar-Terrestrial Physics*, Belgrade, edited by J.W. King and W.S. Newman, p. 91, Academic Press Inc., London.

Elphic, R.C., Weiss, L.A., Thomsen, M.F., McComas, D.J., and Moldwin, M.B.: 1996, 'Evolution of plasmaspheric ions at geosynchronous orbit during times of high geomagnetic activity', *Geophys. Res. Lett.* **23**, 2189–2192.

Gallagher, D.L., Craven, P.D., and Comfort, R.H.: 1998, 'A Simple Model of Magnetospheric Trough Total Density', *J. Geophys. Res.* **103**, 9293.

Gallagher, D.L., Craven, P.D., and Comfort, R.H.: 2000, 'Global Core Plasma model', *J. Geophs. Res.* **105**, 18819.

Gary, S.P., Moldwin, M.B., Thomsen, M.F., and Winske, D.: 1994, 'Hot proton anisotropies and cool proton temperatures in the outer magnetosphere', *J. Geophys. Res.* **99**, 23604.

Goldstein, J., Spasojevic, M., Reiff, P.H., Sandel, B.R., Forrester, W.T., Gallagher, D.L., and Reinisch, B.W.: 2002, 'Identifying the plasmapause in IMAGE EUV data using IMAE RPI in situ steep density gradients', *in press, J. Geophys. Res.*

Grebowsky, J.M.: 1970, 'Model study of plasmapause motion', *J. Geophys. Res.* **75**, 4329.

Gringauz, K.I.: 1963, 'The structure of the ionized gas envelope of earth from direct measurements in the U.S.S.R. of local charged particle concentrations', *Planet. Space Sci.* **11**, 281.

Higel, B., and Lei, W.: 1984, 'Electron density and plasmapause characteristics at 6.6 RE: A statistical study of the GEOS 2 Relaxation sounder data', *J. Geophys. Res.* **89**, 1583.

Horwitz, J.L., Menteer, S., Turnley, J., Burch, J.L., Winningham, J.D., Chappell, C.R., Craven, J.D., Frank, L.A., and Slater, D.W.: 1986, 'Plasma boundaries in the inner magnetosphere', *J. Geophys. Res.* **91**, 8861.

Kozyra, J.U., Jordanova, V.K., Horne, R.B., and Thorne, R.M.: 1995, 'Interaction of ring current and radiation belt protons with ducted plasmaspheric hiss 2. Time evolution and distribution function', *J. Geophys. Res.* **100**, 21911.

Lambour, R.L., Weiss, L.A., Elphic, R.C., and Thomsen, M.F.: 1997, 'Global modeling of the plasmasphere following storm sudden commencements', *J. Geophys. Res.* **102**, 24351–24368.

LeDocq, M.J., Gurnett, D.A., and Anderson, R.R.: 1994, 'Electron Number Density Fluctuations Near the Plasmapause Observed by the CRRES Spacecraft', *J. Geophys. Res.* **99**, 23,661.

Lemaire, J.: 1976, 'Steady state plasmapause positions deduced from McIlwain's electric field models', *J. Atmos. Terr. Physics* **38**, 1041–1046.

Lemaire, J., and Gringauz, K.I.: 1998, 'The Earth's Plasmapause', Cambridge University Press, Cambridge, 350 pp.

Maynard, N.C., and Grebowsky, J.M.: 1977, 'The plasmapause revisited', *J. Geophys. Res.* **82**, 1591.

Maynard, N.C., Denig, W.F., and Burke, W.: 1995, 'Mapping ionospheric convection patterns to the magnetosphere', *J. Geophys. Res.* **100**, 1713–1721.

McComas, D.J., Bame, S.J., Barraclough, B.L., Donart, J.R., Elphic, R.C., Gosling, J.T., Moldwin, M.B., Moore, K.R., and Thomsen, M.F.: 1993, 'Magnetospheric plasma analyzer (MPA): Initial three-spacecraft observations from geosynchronous orbit', *J. Geophys. Res.* **98**, 13453.

Moldwin, M.B., Thomsen, M.F., Bame, S.J., McComas, D.J., and Moore, K.R.: 1994, 'The structure and dynamics of the outer plasmasphere: A multiple geosynchronous satellite study', *J. Geophys. Res.* **99**, 11475.

Moldwin, M.B., Thomsen, M.F., McComas, D.J., Bame, S.J., and Reeves, G.D.: 1995, 'The fine scale structure of the outer plasmasphere', *J. Geophys. Res.* **100**, 8021.

Moldwin, M.B., Downward, L., Rassoul, H.K., Amin, R., and Anderson, R.R.: 2002, 'A new model of the location of the plasmapause: CRRES results', *J. Geophys. Res.*, in press.

Nishida, A.: 1966, 'Formation of plasmapause, or magnetospheric plasma knee, by the combined action of magnetospheric convection and plasma escape from the tail', *J. Geophys. Res.* **71**, 5669.

Sandel, B.R., King, R.A., Forrester, W.T., Gallagher, D.L., Broadfoot, A.L., and Curtis, C.C.: 2001, 'Initial results from the IMAGE Extreme Ultraviolet Imager', *Geophys. Res. Lett.* **28**, 1439–1442.

Sheeley, B.W., Moldwin, M.B., Rassoul, H.K., and Anderson, R.R.: 2001, 'An empirical plasmasphere and trough density model: CRRES Observations', *J. Geophys. Res.* **106**, 25631.

Takahashi, K., and Anderson, B.J.: 1992, 'Distribution of ULF Energy (f<80 mHz) In The Inner Magnetosphere: A Statistical Analysis of AMPTE CCE Magnetic Field Data', *J. Geophys. Res.* **97**, 10751.

Thorne, R.M., and Horne, R.B.: 1992, 'The contribution of ion-cyclotron waves to electron heating and SAR-arc excitiation near the storm-time plasmapause', *Geophys. Res., Lett.* **19**, 419.

Webb, D., and Orr, D.: 1975a, 'Spectral Studies of Geomagnetic Pulsations with Periods Between 20 and 120 sec And Their Relationship to the Plasmapause Region', *Planet Space Sci.* **23**, 1551.

Webb, D., and Orr, D.: 1975b, 'Statistical Studies of Geomagnetic Pulsations with Periods Between 20 and 120 sec And Their Relationship to the Plasmapause Region', *Planet Space Sci.* **23**, 1169.

Wilson, G.R., Horwitz, J.L., and Lin, J.: 1992, 'A Semikinetic Model for Early Stage Plasmasphere Refilling 1. Effects of Coulomb Collisions', *J. Geophys. Res.* **97**, 1109.